MEASUREMENTS AND PREDICTIONS OF ROOM AIRFLOW PATTERNS USING DIFFERENT TURBULENCE MODELS

D. Müller, U. Renz

Lehrstuhl für Wärmeübertragung und Klimatechnik (WÜK)
RWTH-Aachen, Germany

ABSTRACT

To evaluate the performance of different turbulence models in room airflow applications measurements in a test room will be compared to numerical calculations. The measurements are taken in a 6 x 4 x 3 m^3 room with two heated dummies and a computer. Zero heat flux boundary conditions are achieved by controlling the inner and outer wall temperature. Two different ventilation systems will be examined in order to get momentum and buoyancy driven flow fields. Temperature measurements and Particle Streak Tracking data will be compared to the numerical predictions.

The standard k, ε - model, a low Reynolds model and a Reynolds stress model will be used to get an overview about their applicability to different ventilation systems.

KEYWORDS

Air flow pattern, Boundary layer, CFD, Displacement ventilation.

INTRODUCTION

The use of numerical calculations (CFD) to evaluate different ventilation systems becomes a common tool for the planning of new buildings or the enhancement of the energy economy of old buildings. Different studies in the past show successful calculations of the airflow patterns in buildings as well as poor agreement between calculated and measured data. It is almost impossible to get good measurements of the airflow pattern in real buildings for two main reasons. First of all it is very difficult to measure all boundary conditions of an enclosure such as wall temperature, inlet velocities and turbulence quantities, infiltration and all heat source characteristics. Additionally, most measurement methods record airflow velocities or air temperatures only at a few locations inside an enclosure. To get an overview of the airflow pattern in the room or at least in one or two planes inside the enclosure it is necessary to record data for a long time because every location needs to be evaluated for a reasonable averaging time. During this time the boundary conditions will not remain constant due to changing environment conditions like the outside temperature and radiation load.

This study uses a test room to guarantee constant conditions for the measurement period. The room is located inside a larger enclosure to control all wall temperatures of the small room. Two different air distribution systems are installed for the measurement period. The air flow pattern at two planes and the temperature profile at two locations are measured for a ceiling slot and a displacement ventilation system.

EXPERIMENTAL SET-UP

The test room and the large enclosure are connected to a common air condition system. The temperature of the outer enclosure is controlled by an additional heating system to achieve the same temperatures as measured in the inner room. To minimise the heat loss through the wall the inner chamber is insulated. The test room has two different inlet devices, two dummies and a computer model. Both dummies and the computer have an electrical heating system. One dummy transfers 100 W by convection and radiation to the room. The computer produces 200 W leading to 400 W overall heat load. The volume flow of the inlet and outlet air is controlled by two separate fans and both volume flows are measured by orifice plates. The volume flow rate was set to three air exchange rates for all ventilation systems. The inlet velocities were measured using a hot wire anemometer and the flow direction was estimated with smoke experiments.

MEASUREMENT METHODS

Temperature Measurements

The room air temperature profiles are measured with 24 thermocouples on two room locations at 12 different room heights. One profile shows the temperature distribution at the centre of the empty room half (Pos. 1) and the other profile is located at the centre of the table between the two dummies (Pos. 2). Also, the inlet temperature as well as the four outlet temperatures are measured and all measurements are recorded vs. time. During the measurement period the heat loss of the test room was below 10% of the internal heat load.

Velocity measurements

For the velocity measurements a Particle-Streak-Tracking (PST) system is used. A description of the system is given by Müller (1998) and is presented during Roomvent '98.

CFD-CALCULATIONS

All CFD-calculations based on the FLUENT code use a body fitted three dimensional grid with small modifications to account for the three inlet systems. The grids have 50,000 to 60,000 cells concentrated at the heat sources in the right room side and the inlet devices. The grid is a compromise between the calculation time and the flow field resolution.

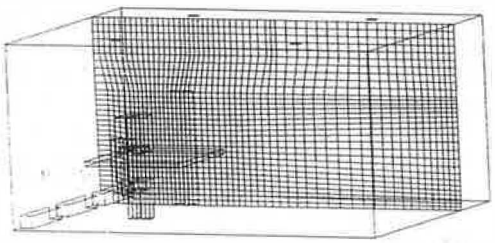

Figure 1 Body fitted CFD grid, displacement ventilation system

The average cell volume is 0.001 m^3. Grid independence was not checked because to prove grid independence of the solution it would be reasonable to generate a grid using one half node distance yielding to a grid size of 500,000 cells.

BOUNDARY CONDITIONS

The average inlet velocity was measured for all ventilation systems. Every grid matches the inlet geometry yielding to the correct formulation of the average momentum of each inlet system. The following table shows the inlet boundary conditions for both test cases.

Table 1 Measured inlet boundary conditions

Inlet device system	*Average velocity [m/s]*	*Flow angle - ceiling*
Slot diffuser	2.1 - 2.75	18°
Displacement Ventilation	0.1	0°

The inlet turbulence boundary condition is estimated with respect to the inlet geometry as the hydraulic diameter.

Table 2 Inlet boundary conditions

Inlet device system	*Turbulence intensity*	*Turbulence length scale*
Slot diffuser	10%	5 mm
Displacement Ventilation	5%	35 mm

One dummy transfers 100 W into the chamber. The radiation heat transfer is estimated to 50 W based on surface temperature measurements leading to 50 W convective heat transfer of each dummy. The computer produces 100 W of thermal energy and has a cooling fan. The computer model uses an outlet cell for the mass flux going into the computer and one inlet cell to simulate the fan. The mass flow and the temperature difference between inlet and outlet matches the real set-up leading to 80 W thermal energy. The rest of the thermal energy is transferred by convection and radiation on the computer surface.

The monitor model uses heat flux boundary conditions to transfer 60 W on the vertical surfaces into the chamber and 40 W are transferred by radiation. A heat flux condition on horizontal surfaces of the monitor model would lead to an unreasonable high turbulence production due to the buoyancy source term. The radiation load is assumed to be uniform on all inner walls and the desk surface.

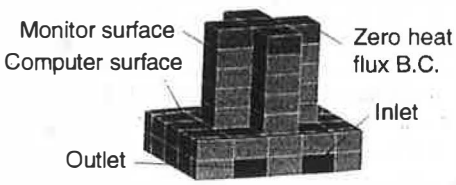

Figure 2 Monitor and computer model

TURBULENCE MODELS

The velocity field of a turbulent flow is fully described by the time dependent Navier-Stokes equations.

$$\frac{\partial}{\partial t}(\rho u_i) + \frac{\partial}{\partial x_i}(\rho u_i u_j) = \frac{\partial}{\partial x_j}\left(\eta\left(\frac{\partial u_i}{\partial x_j} + \frac{\partial u_j}{\partial x_i}\right) - \left(\frac{2}{3}\eta\frac{\partial u_k}{\partial x_k}\right)\right) - \frac{\partial p}{\partial x_i} + \rho g_i + F_i - \frac{\partial}{\partial x_j}\left(\rho\overline{u_i' u_j'}\right)$$

The last term of this equation, the Reynolds stresses, has to be modelled using time averaged velocity gradients to close the equation system.

Two equation turbulence model

For a linear two equation turbulence model this term is usually calculated applying the eddy viscosity model.

$$\left(\rho\overline{u_i' u_j'}\right) = \rho\frac{2}{3}k\,\delta_{ij} - \eta_t\left(\frac{\partial u_i}{\partial x_j} + \frac{\partial u_j}{\partial x_i}\right) + \frac{2}{3}\eta_t\frac{\partial u_i}{\partial x_i}\delta_{ij}$$

The turbulent viscosity η_t couples the velocity gradients to the unknown Reynolds stresses and it works as an additional local viscosity of the fluid.

$$\eta_t = \rho\, f_\eta\, C_\eta \frac{k^2}{\varepsilon}$$

The function f_η describes the influence of wall damping effects and might be used to model relaminarisation effects in low Reynolds number flows. For large turbulent Reynolds numbers and in the standard k, ε - model f_η is equal to unity. To calculate the turbulent viscosity η_t it is necessary to solve a transport equation for the kinetic energy k and the dissipation of the kinetic energy ε.

$$\frac{\partial}{\partial t}(\rho k) + \frac{\partial}{\partial x_i}(\rho u_i k) = \frac{\partial}{\partial x_i}\left(\eta + \frac{\eta_t}{\sigma_k}\right)\frac{\partial k}{\partial x_i} + P_k + G_b - \rho\varepsilon$$

$$\frac{\partial}{\partial t}(\rho\tilde{\varepsilon}) + \frac{\partial}{\partial x_i}(\rho u_i\tilde{\varepsilon}) = \frac{\partial}{\partial x_i}\left(\eta + \frac{\eta_t}{\sigma_\varepsilon}\right)\frac{\partial\tilde{\varepsilon}}{\partial x_i} + C_{1\varepsilon}\frac{\tilde{\varepsilon}}{k}\left(P_k + (1-C_{3\varepsilon})G_b\right) - f_{2\varepsilon}C_{2\varepsilon}\rho\frac{\tilde{\varepsilon}^2}{k} + E$$

$$\varepsilon = \tilde{\varepsilon} + D \;;\; D = 2\eta\left(\frac{\partial\sqrt{k}}{\partial x_i}\right)^2 \;;\; E = 2.0\,\frac{\eta\eta_t}{\rho}\left(\frac{\partial^2 u_i}{\partial x_k \partial x_l}\right)^2$$

The terms D and E are part of the low Reynolds turbulence model proposed by Launder and Sharma (LS) and vanish for the standard k, ε - model formulation. The term P_k is the production term of turbulence energy due to shear stress effects and G_b describes the production rate due to buoyancy effects. G_b plays an important role in room airflows because of the very low production term due to shear stresses far away from air supplies and heat sources and it will be modelled using the gradient - flux principle. Different values are proposed for the constant $C_{3\varepsilon}$ in the literature. This study will test the values 0, 0.55 and 1 for $C_{3\varepsilon}$.

$$P_k = \eta_t\left(\frac{\partial u_i}{\partial x_j} + \frac{\partial u_j}{\partial x_i}\right)\frac{\partial u_i}{\partial x_j} \;;\; G_b = -g_i\frac{\eta_t}{\rho Pr_t}\frac{\partial\rho}{\partial x_i}$$

The temperature gradient will control the turbulence production and dissipation in the large empty space of an enclosure. For large turbulent Reynolds numbers and the standard k, ε - model f_η and $f_{2\varepsilon}$ are equal to unity. The LS model gives the following functions for f_η and $f_{2\varepsilon}$ describing the effects of a low turbulent Reynolds number Re_t.

$$f_\eta = \exp\left[-3.4\,/\left(1+\frac{Re_t}{50}\right)^2\right] \;;\; f_{2\eta} = 1 - 0.3\exp\left[-Re_t^2\right]$$

One advantage of using the LS model for room airflows is that all turbulence damping effects depend on the turbulent Reynolds number Re_t and not on a wall distance parameter.

$$Re_t = \frac{\rho k^2}{\varepsilon\eta} \neq f(y^+)$$

Thus, the model can be used far away from walls but it is still not verified for this flow region. The model has to be judged by comparison to experimental data. The standard k, ε - model is implemented in FLUENT and the LS model was implemented at WÜK by Vogl (1997).

The Reynolds stress model (RSM)

FLUENT uses the following equations to calculate the Reynolds stresses.

$$\frac{\partial}{\partial t}\left(\rho\overline{u_i' u_j'}\right) + u_k\frac{\partial}{\partial x_k}\left(\rho\overline{u_i' u_j'}\right) =$$

Diffusive Transport: $+\frac{\partial}{\partial x_k}\left(\frac{\eta_t}{\sigma_k}\frac{\partial\overline{u_i' u_j'}}{\partial x_k}\right)$

Production: $-\left[\overline{u_i' u_k'}\frac{\partial u_j}{\partial x_k} + \overline{u_j' u_k'}\frac{\partial u_i}{\partial x_k}\right]$

Press.-Strain: $-C_1\frac{\varepsilon}{k}\left(\rho\overline{u_i' u_j'} - \rho\frac{2}{3}k\,\delta_{ij}\right) - C_2\left(P_{ij} - \frac{1}{3}P_{ii}\,\delta_{ij}\right)$

Dissipation: $-\frac{2}{3}\delta_{ij}\varepsilon$; $P_{ij} = -\rho\overline{u_i' u_k'}\frac{\partial u_j}{\partial x_k} - \rho\overline{u_j' u_k'}\frac{\partial u_i}{\partial x_k}$

The transport equation for ε is identical to the standard k, ε - model formulation assuming isotropic dissipation of the turbulent energy. Now five additional transport equations have to be solved yielding to a certain increase of the calculation time. Also, all higher correlations are approximated by relations using velocity gradients from the time averaged flow field as the k, ε - models.

RESULTS

Slot ventilation system

The temperature measurements during 5 hours are averaged and corrected with the 10% heat loss through the chamber walls. Figure 3 shows the measured and calculated temperature profile at position 1 (centre empty space of the room) and position 2 (centre of the space with heat sources).

The standard k, ε - model shows the best agreement with the measured temperature profile at position 1. The low Reynolds model overpredicts the mixing of the inlet jet and the warmer room air yielding to a larger temperature at the ceiling. The Reynolds stress model underestimates the turbulence level at the inlet jet leading to a cold jet at the ceiling. The measured temperature profile at position 2 shows larger temperatures over the desk than all calculation results. The transport of the warm air from all heat sources to the desk centre is larger than the calculated transport. The Reynolds stress model shows the best agreement to the measured data at position 2.

A variation of the constant C_{μ} has a negligible effect on the solution of the two equation turbulence models.

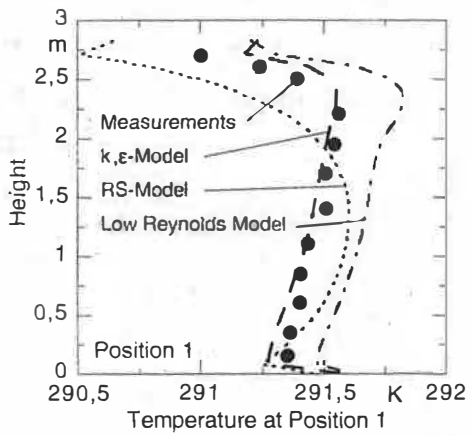

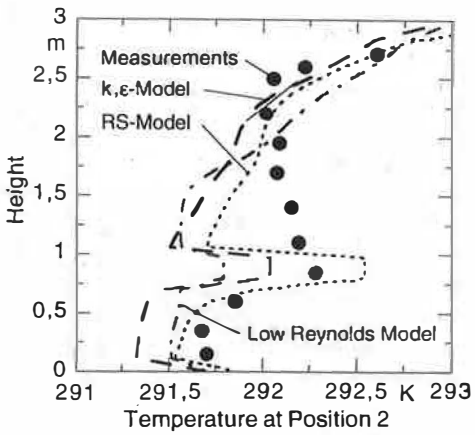

Figure 3 Temperature profiles

Velocity measurements

The velocitieswere measured in two planes (x=1.5 m; y=1.5m) using the PST system. Both planes were divided in smaller measurement planes and many PST pictures with different pulse times were evaluated in each plane. To compare the PST data to CFD results the velocities in the first plane are evaluated at 450 room locations by local weighted averaging of over 24,000 velocity vectors.

Figure 4 shows the comparison of the measured data to the CFD calculation results applying different turbulence models. All CFD results show a curved plume over the sitting dummy heat source. The curvature is caused by the large room vortex that carries the inlet momentum of the flow to the lower right side of the enclosure. The PST measurements show lower velocities close to the walls in combination with a larger region of almost constant velocities at the upper right room half. The measurements show no influence of the large room vortex close to the left wall and thus, the free convection flow over the dummy shows no curvature.

The temperature profile at position 1 can be explained by the airflow pattern. The low Reynolds model predicts a larger velocity components towards the top wall in the upper room half. This leads to a fast temperature increase in the inlet jet region. The Reynolds stress model shows high flow velocities close to the top wall caused by the lowest near wall turbulent viscosity resulting in too low temperatures. The amount of measured velocity vectors does not allow to determine statistical values of the flow ve-

locities at this plane. It was not possible to get a stationary solution for the CFD calculation. The time dependent CFD results show the time averaged velocities for each time step. The evaluation of the time dependent velocities shows a small change of all velocity components over the heat sources caused by a frequent variation of the free convection flow direction. All calculation results show a reasonable agreement with the measurements.

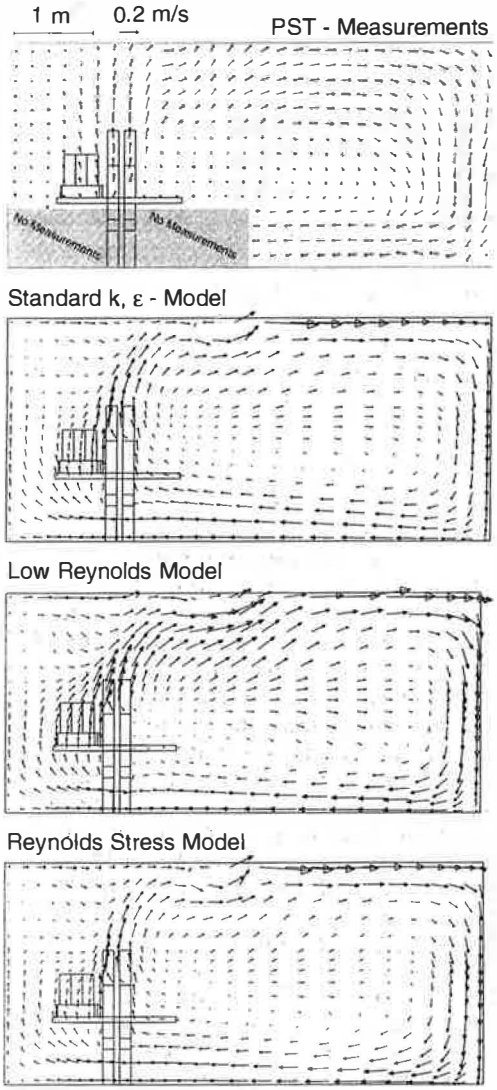

Figure 4 Airflow pattern at x = 1.5 m

The second measurement plane is located at the centre of the heated room half (y=1.5 m). Both dummies and the desk are located inside this plane. The measured airflow pattern shows smaller velocities above both dummies and a stronger flow from the left dummy to the desk centre. This could be the reason for the difference between the measured and calculated temperature profiles at position 2. The free convection airflow caused by the computer heat sources has a strong influence on the calculated airflow pattern because of the curved flow towards the room centre. The measurements do not show any upward moving flow in this flow region.

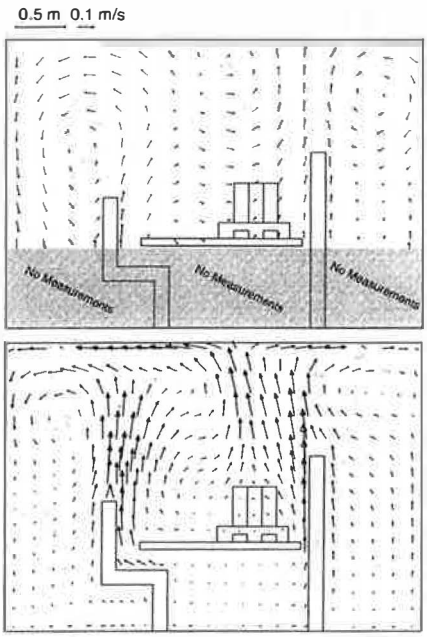

Figure 5 Airflow pattern at y = 1.5 m, measurements and k, ε - model

Displacement ventilation system

Assuming a uniform radiation distribution from the heat sources and neglecting the radiative heat transfer from wall to wall (radiation model 1) results in wrong temperature profiles.

All numerical calculations using different turbulence models overpredict the temperature gradient in the enclosure. To estimate the radiation heat transfer the discrete transfer model is used. Every wall cell emits a certain number of rays and applies a radiation balance with every target wall cells of the rays. The two dummies have a small surface compared to the wall and a large number of rays would be necessary to ensure that every wall cell hits both dummy surfaces. The computer model can not account for the additional surface by fins and thus, the surface temperature of the computer model has a high unrealistic value. To

solve this problem the view factors for the heat sources are estimated and only the radiation heat transfer of the walls and the desk is calculated using the discrete transfer model, see figure 7.

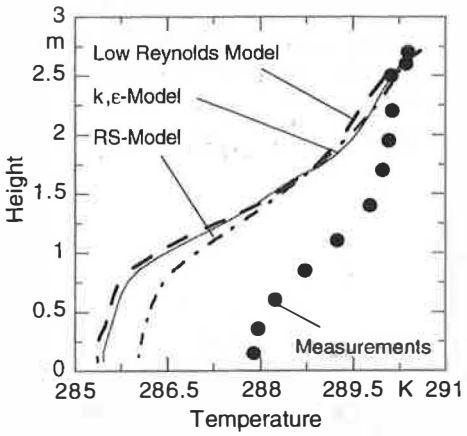

Figure 6 Temperature profiles at pos. 1 (equal radiation distribution)

The main heat flux is emitted from the bottom wall and the top wall has almost a zero heat flux condition. This result neglects the fact that the heat transfer estimated applying a wall function which is not valid for a mixed convection flow situation.

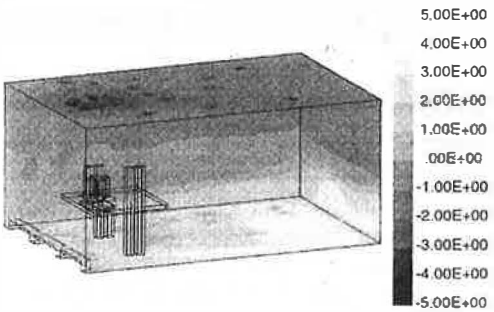

Figure 7 Calculated wall heat flux in the enclosure [W/m^2]

Nevertheless, to save computer time all CFD calculations for the displacement ventilation system have a heat flux boundary condition at the bottom wall to account for all the radiation heat flux inside the enclosure (radiation model 2). Figure 8 shows the temperature profiles for this new radiation boundary condition.

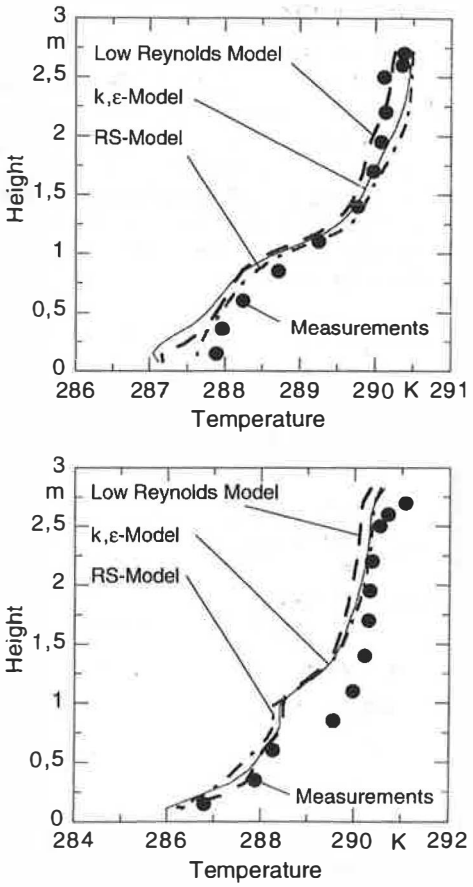

Figure 8 Temperature profiles at position 1 & 2 accounting for radiation heat transfer

The radiation heat transfer between the top and the bottom wall of the enclosure is able to decrease the temperature gradient and leads to a good agreement between the measurements and the calculation results. A similar result was reported by Jacobsen (1993). A variation of the constant C_ε (0, 0.55, 1) in the dissipation equations shows only a small influence on the temperature profile in the enclosure.

Velocity measurements

The velocities were measured in two planes (x = 1,5 m and y = 1.5 m) using the PST system.

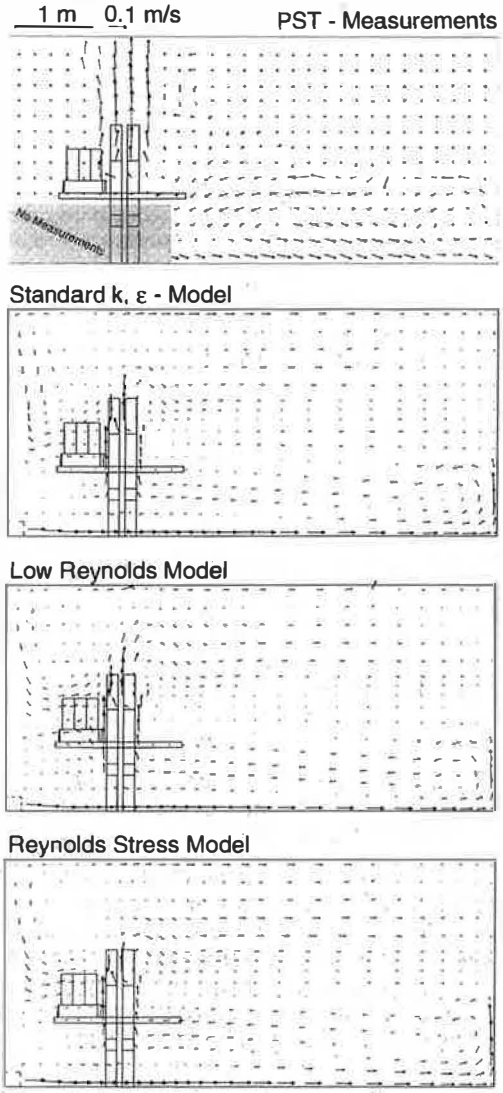

Figure 9 Airflow pattern at x = 1.5 m

Two planes were divided in smaller measurement planes and many PST pictures with different pulse times were evaluated in each plane. To compare the PST data to CFD results the velocities in the planes are local weighted averages. Figure 9 shows the comparison of the measured data to the CFD calculation results applying different turbulence models at x=1,5m.

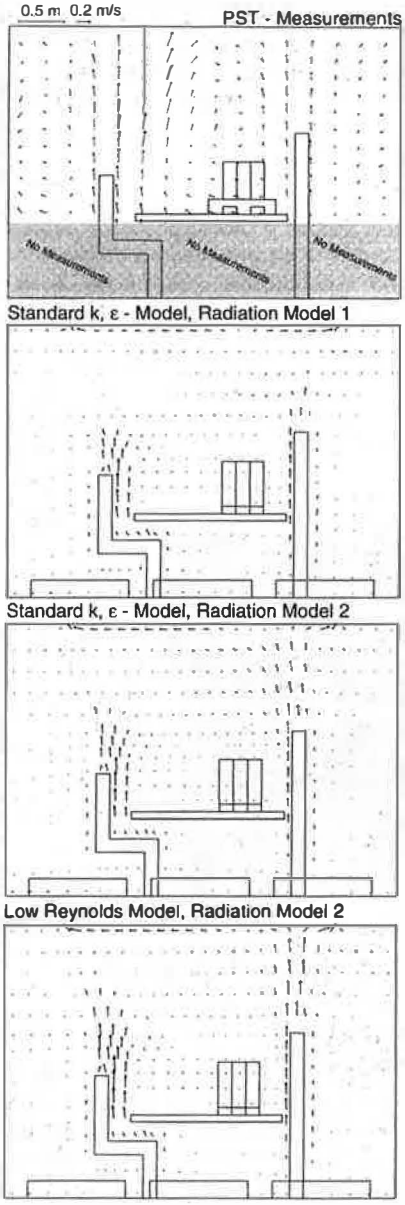

Figure 10 Airflow patterns at y=1.5m

The CFD calculations do not show the buoyancy driven plume over the sitting dummy as the measurements do. The low Reynolds model predicts the strongest plume resulting in the best agreement with the measured temperature profile. The measured airflow pattern shows a return flow from the right wall of the enclosure and a mixing process in the shear layer between the return and the inlet flow. The calculation results predict much lower velocities in the return flow region.

Figure 10 shows the airflow patterns at y=1.5m for the standard k, ε - model applying the radiation model 1 and 2 and the low Reynolds solution using radiation model 2.

The large temperature gradient for radiation model 1 causes a fast disintegration of the buoyancy plumes over both dummies. Radiation model 2 in combination with the standard k, ε - model gives a rising plume only over the standing dummy and a weak plume over the sitting dummy. The low Reynolds model predicts a lower effective viscosity of the fluid resulting in a slower decrease of the temperature difference between the plumes and the environment air, see figure 11. This fact leads to the best agreement with the measured airflow velocities.

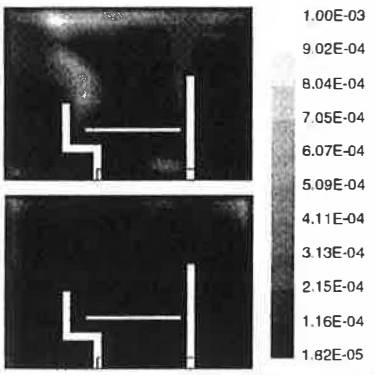

Figure 11 Calculated effective viscosity for the standard and low Reynolds k, ε - model [kg/m s]

DISCUSSION

The CFD calculation results for the slot ventilation system are in good agreement with the measured air temperature profiles and airflow pattern. All buoyancy plumes rise to the ceiling because of the small temperature gradient in the enclosure. The flow is dominated by the inlet momentum flux and the buoyancy terms in the turbulence model have only a small effect on the flow field.

To calculate the displacement ventilation system it is very important to estimate radiation boundary conditions carefully. If the temperature gradient increases during the iteration process the buoyany term in the turbulence model will decrease the mixing process resulting in a further increase of the temperature gradient in the enclosure. For example, the CFD results show a too large temperature gradient in the room assuming a uniform radiation load distribution. The radiation heat transfer can be calculated using the discrete transfer model. To save computer time and storage it is reasonable to estimate the radiation flux from the small heat sources applying view factors. The discrete transfer model gives a good accuracy for surfaces with an comparable area. Using modified boundary conditions with respect to radiations gives a good agreement of the temperature profiles with the measurements. The plumes over the sitting dummy do still not rise to the top of the enclosure caused by the turbulence models and the grid resolution. The low Reynolds model of Launder-Sharma shows the best overall agreement with the measurements.

To improve the accurracy of the radiation heat transfer calculations it is necessary to account for the effects in the boundary layer. The use of wall functions leads to wrong surface temperatures for mixed and free convection flows and thus, the quality of radiation transfer models is limited by the accuracy of the near wall treatment.

ACKNOWLEDGEMENTS

The excellent support of the student worker Armin Knels is gratefully acknowledged. The responsibility for the content of this paper lies solely with the authors.

REFERENCE

Abrahamson, S. D.; Koga, D. J.; Eaton, J. K. (1988) An Experimental Investigation of the Flow between Shrouded Co-rotating Disks, Report MD-50 of the Thermoscience Division of Mech. Eng. Dept., Stanford University, Stanford, California.

Jacobsen, T. (1993) Airflow and Temperature Distribution in Rooms with Displacement Ventilation, PhD-Thesis, University of Aalborg

Launder, B. E.; Sharma, B.I. (1974) Application of the Energy-Dissipation Model of Turbulence to the Calculation of a Flow near a Spinning Disk, Letters in Heat and Mass Transfer. 1, 131/138

Müller, D.; Renz, U. (1998) A low cost Particle Streak Tracking System (PST) and a new approach to three dimensional Airflow Velocity Measurements, Roomvent '98

Vogl, N. (1996) Numerische Berechnung von auftriebsbeeinflußten Raumluftströmungen, PhD-Thesis, RWTH-Aachen